Available online at www.sciencedirect.com
ScienceDirect
Journal of Sound and Vibration 322 (2009) 926–940
JOURNAL OF SOUND AND VIBRATION
www.elsevier.com/locate/jsvi

Equivalent 'rain on the roof' loads for random spatially correlated excitations in the mid–high frequency range

M.N. Ichchou[a,*], B. Hiverniau[b], B. Troclet[b]

[a] *Université de Lyon, Ecole Centrale de Lyon, 36, avenue Guy de Collongue, 69134 Ecully Cedex, France*
[b] *EADS ST, 66, Route de Verneuil, BP 3002, 78133 Les Mureaux Cedex, France*

Received 4 September 2008; received in revised form 18 November 2008; accepted 25 November 2008
Handling Editor: C.L. Morfey

Abstract

The present paper deals with equivalent "rain on the roof" (ROF) excitations, which allow the modeling of spatially correlated broadband sources by statistically independent point forces. ROF excitation largely simplifies the expressions of the joint acceptance functions and can be easily modeled using

finite element method (FEM). Two approaches are presented here and an equivalent model of excitation is developed and validated on acoustic and aerodynamic excitations, such as diffuse field or turbulent boundary layer (TBL) excitations. The first idea, considers the equivalence over the extended physical domain. It allows equivalent ROF excitation only for frequencies over the acoustic coincidence effect. The second method is based on the wavenumber space equivalence. Validation of this approach has been carried out for different acoustic and aerodynamic excitations, and for different structural boundary conditions. Numerical experiments show that this approach gives acceptable results for a wide frequency range specifically for TBL excitations.

1. Introduction

Broadband and random excitations are relevant in many engineering problems. For instance, launch vehicles are subjected at lift-off and during flight ascent to a severe acoustic and aerodynamic environment which are random in nature. Electronic equipments and satellites are consequently excited and the random vibration levels induced by the acoustic environment must be predicted before flights. The response of fluid loaded structures can be estimated from data on the unsteady pressure field and their correlation functions. In the high-mid frequency range statistical energy analysis (SEA) [1], hybrid FEM/SEA techniques [2] or SEA-like (SEAL) [3,4] are the most considered energy methods in the literature. Joint acceptance functions (expressing to some extent the part of unsteady pressure field energy, which is converted into vibrations) are then the key concern. Closed formulations of theses acceptances functions in the case of standard structures (such as plates and cylinders), can be obtained for use in SEA. However, the computations of these functions

*Corresponding author. Tel.: +33 4 72 18 62 30; fax: +33 4 72 18 91 44.
E-mail address: mohamed.Ichchou@ec-lyon.fr (M.N. Ichchou).

0022-460X/$ - see front matter © 2008 Elsevier Ltd. All rights reserved.
doi:10.1016/j.jsv.2008.11.050

are time consuming in the mid-high frequency range, when finite element method (FEM) of the given structure is used. SEAL [3] can be considered to bridge the gap between low frequency and high frequency analyses. Ref. [3] also offers some theoretical and applicative definitions of the energy methods, and through the concept of energy distribution approach justifies also some 'inconsistencies' of the standard SEA approach. A key concept in SEAL formulation [3,4] is the energy influence coefficients (EIC). To compute such EIC the FEM of the structure is excited by rain on the roof (ROF) excitations. One of the main difficulties lies then in the modeling of *real excitations* encountered such as aerodynamic and diffuse noises.

The aim of the present paper is to define equivalent ROF excitations for spatially correlated sources to be used in mid-high frequency vibroacoustic predictions [5]. Many studies [6–13] have considered spatially correlated acoustic and aerodynamic excitations. Most of them were carried out in order to estimate the spatial correlation function for specific excitations. Aerodynamic loads are often represented by empirical models of correlation functions provided by experimental measurements [7–9] and [12,13]. Most recent studies about spatially correlated excitations focus on the representation of the power spectral density of response in the wavenumber space [14–16]. The method expresses all modal expansion terms in the wavenumber space and has two main advantages. The expressions in the wavenumber space allow a better understanding of different modes contributions to the total response of the structure to an incident pressure field. The second aspect is connected to time-consumption, since correlation functions have lower variations in the wavenumber space, joint acceptance computation time is reasonable when compared to the space–frequency representation. It should be noted that some numerical advances in the derivation of random vibration was recently presented [17]. Specific approximations referring to the meshing condition and to the transformation of the distributed excitation, as well as a numerical scheme named asymptotic scaled modal analysis was introduced. The work [17] demonstrates that FEM can be used in the random vibration predictions without increasing the computational costs.

The present study is performed assuming that the correlation function of the excitation sound field under interest is known and well described. ROF excitations, equivalent to the acoustic and aerodynamic excitation of interest, are developed. An existing equivalent model was presented in the literature by Maidanik [10]. This model has been validated on aerodynamic excitations encountered in the aerospace industry. This model is called spatial extent equivalence and has been studied more deeply in Ref. [11]. The present paper demonstrates that this approach is not sufficient, and a second model, called *wavenumber space equivalence*, is then developed. Different random broadband noises are then investigated, and a wavenumber space equivalence model is validated for different excitations cases. The generality of the proposed equivalence is also considered. Indeed, different structural boundary conditions are used in order to check the feasibility. The paper is then structured as follows. Section 2 provides basic concepts concerning random vibration characterization and describes random excitations under interest. Section 3 is devoted to the equivalent ROF excitations analysis. Section 3 gives also some numerical interrogations to evaluate the proposed approach accuracy.

2. Characterization of random broadband excitations

Standard approaches used to predict vibration levels under random pressure fields are often based on modal decomposition. The response to a broadband random noise is expressed in terms of power spectral density. Statistical considerations are then introduced, and power spectral density is deduced from the correlation function which is defined in what follows as

$$R_{pp}(\boldsymbol{\xi},\tau) = E[p(\mathbf{x};t)p(\mathbf{x}+\boldsymbol{\xi};t+\tau)] \tag{1}$$

with $\boldsymbol{\xi} = \mathbf{x}'-\mathbf{x}$ the spatial separation vector, τ the time shift and E the mathematical expectation. In this paper, the stochastic field $p(\mathbf{x};t)$ is assumed to be homogenous. The space-frequency spectrum can then be written as follows:

$$S_{pp}(\boldsymbol{\xi};\omega) = \int_{-\infty}^{\infty} R_{pp}(\boldsymbol{\xi};t)\,\mathrm{e}^{-\mathrm{j}\omega t}\,\mathrm{d}t \tag{2}$$

The power spectral density of structural motion is estimated from the pressure field considered in terms of blocked pressure. This corresponds to the fact that the wall-pressure fluctuations are not affected by the structural vibration. The pressure field is then the same as observed on a rigid wall. The power spectral density of velocity of a structure submitted to random excitations can be expressed as follows from the generalized Green functions:

$$S_{vv}(x,y;\omega)=\omega^2\sum_r\sum_s \mathrm{Re}(\alpha_r(\omega)\alpha_s^*(\omega))\Phi_r(x,y)\Phi_s(x,y)\int_A\int_A \Phi_r(x,y)\Phi_s(x',y')S_{pp'}(\omega)\,\mathrm{d}A\,\mathrm{d}A' \tag{3}$$

Φ_r is the mode shape of the excited structure, Rethe real part of the complex number, $S_{pp'}$ the cross-spectral density of the wall pressure, A the area excited by the pressure field and α_r the modal receptance of the structure

$$\alpha_r(\omega)=\frac{1}{\omega_r^2(1+\mathrm{i}\eta_r)-\omega^2} \tag{4}$$

ω_r is the pulsation of the mode r and η_r the associated damping loss factor. The cross-spectral density of the wall pressure between two excitation points of the structure can be expressed as follows:

$$S_{pp'}(\omega)=C(P,Q;\omega)S_{pp}(\omega) \tag{5}$$

where C is the correlation function of the pressure field and S_{pp} the point power spectral density of the pressure field, assumed to be constant over the surface of the structure. We notice here that the correlation function is only dependent on the frequency and the distance between the given points P and Q. This correlation function is generally expressed by analytical formulations with coefficients derived from experimental data for a given excitation. Consequently, the power spectral density of velocity averaged over space domain (D) and frequency ($\Delta\omega$) is

$$\langle S_{vv}\rangle_{\Omega,\Delta\omega}=\frac{1}{\Delta\omega}\int_{\Delta\omega}\int_D \omega^2\sum_r\sum_s \mathrm{Re}(\alpha_r(\omega)\alpha_s^*(\omega))\Phi_r(x,y)\Phi_s(x,y)A^2S_{pp}(\omega)j_{rs}(\omega)\,\mathrm{d}S\,\mathrm{d}\omega \tag{6}$$

The joint acceptance function j_{rs} has been introduced above, and is computed performing a double integration of the product of the correlation function and the mode shapes of the structure over the surface of the structure:

$$j_{rs}(\omega)=\frac{1}{A^2}\int_A\int_A \Phi_r(x,y)\Phi_s(x',y')C(x-x',y-y';\omega)\,\mathrm{d}x\,\mathrm{d}x'\,\mathrm{d}y\,\mathrm{d}y' \tag{7}$$

Different excitation models can be compared in terms of mean joint acceptance function over resonant modes, as done in the high frequency approach [18]. Indeed, total mean energy of an SEA subsystem excited by a spatially correlated excitation is expressed as follows:

$$\langle S_E\rangle=\langle j_{mm}(\omega)\rangle\sum_m\frac{1}{\Delta\omega}\int_{\Delta\omega}\omega^2|\alpha_m(\omega)|^2A^2S_{pp}(\omega)\,\mathrm{d}\omega \tag{8}$$

$\langle j_{mm}(\omega)\rangle$ is the average of the joint acceptance functions over the resonant modes in the considered frequency band. In order to simplify the expression and the post processing, simply supported plates are considered here, as often in the literature. The joint acceptance functions can then be written in an analytical way for comparisons issue mainly. Three types of excitations are investigated in this paper: the purely random noise, the incident diffuse field, the turbulent fluctuations of wall pressure. ROF excitation is then considered as a reference and all other types of excitations are then derived.

2.1. Purely random excitation

Purely random excitation corresponds to a white noise in the wavenumber space. It can be defined from a spatially delta-correlated function from one point to another:

$$C(x-x',y-y';\omega)=\delta(x-x')\delta(y-y') \tag{9}$$

where δ is the delta function. The use of this type of correlation function allows us to simplify the modal expression of the power spectral density of the response. Indeed, for local mode shapes over the area A, and considering the normalization to 1 of the orthogonal basis of the mode shapes

$$\int_A \Phi_r(x,y)\Phi_s(x,y)\,\mathrm{d}x\,\mathrm{d}y = \delta_{rs} \tag{10}$$

The joint acceptance functions can be expressed explicitly as follows:

$$j_{rs}(\omega) = \frac{1}{A^2}\int_A\int_A \Phi_r(x,y)\Phi_s(x',y')\delta(x-x')\delta(y-y')\,\mathrm{d}x\,\mathrm{d}x'\,\mathrm{d}y\,\mathrm{d}y' \tag{11}$$

$$j_{rs}^{\mathrm{rain}}(\omega) = \frac{\delta_{rs}}{A^2} \tag{12}$$

This relation simplifies the modal summation and leads to the following expression of the power spectral density:

$$S_{vv}^{\mathrm{PR}}(x,y;\omega) = \omega^2 \sum_r |\alpha_r(\omega)|^2 \Phi_r^2(x,y) S_{pp}(\omega) \tag{13}$$

According to previous simplifications, standard vibroacoustic methods are validated under the hypothesis of a ROF excitation. In order to use such methods, equivalent ROF excitations for every spatially correlated loading case are developed in the next section. This equivalent model enables us to represent aerodynamic loading from a spatially delta-correlated excitation, and to use all developments obtained under the hypothesis of ROF excitation. The correlation functions can be defined in the wavenumber–frequency spectrum from the space–frequency spectrum as follows:

$$C(k_x,k_y;\omega) = \frac{1}{(2\pi)^2}\int\int_\infty C(\zeta,\chi;\omega)\,\mathrm{e}^{-\mathrm{i}k_x\zeta-\mathrm{i}k_y\chi}\,\mathrm{d}\zeta\,\mathrm{d}\chi \tag{14}$$

k_x and k_y are the wavenumbers in the two directions, $\zeta = x-x'$ and $c = y-y'$. In most cases, this formulation gives relatively simple expressions of the correlation functions. The expression of the ROF correlation function in the wavenumber space requires that the energy be uniformly distributed over the entire wavenumber–-frequency range, given that the density is uniform over the entire area:

$$C(k_x,k_y;\omega) = \frac{1}{4\pi^2} \tag{15}$$

The energy of the pressure field is uniformly distributed over the entire wavenumber-frequency range, which implies that the mean-square pressure is infinite. In practice, to overcome this difficulty, the ROF excitation is approximated by an ideal low-pass process described by a uniform spectral density defined over a limited wavenumber band [14].

2.2. Incident diffuse field

The incident diffuse field is represented by an infinite sum of uncorrelated plane waves whose incidence angles are uniformly distributed over a half-space. The correlation function is given in the space–frequency domain by

$$C(x-x',y-y';\omega) = \frac{\sin(k_0(x-x'))}{k_0(x-x')}\frac{\sin(k_0(y-y'))}{k_0(y-y')} \tag{16}$$

k_0 is the acoustical wavenumber given by $k_0 = \omega/c_0$, with c_0 the speed of sound, and $x-x'$ and $y-y'$ the distances between the two excitation points. For an incident diffuse field, representation of the correlation function in the wavenumber space is

$$C(k_x,k_y) = \frac{1}{4k_0^2} \quad \text{if } |k_x|<k_0 \text{ and } |k_y|<k_0$$

$$C(k_x,k_y) = 0 \quad \text{else} \tag{17}$$

This expression implies that acoustically slow modes ($|k_x|>k_0$ and $|k_y|>k_0$) do not respond to an incident diffuse field. In practice, these modes respond in the form of corner modes [6]. The last excitation type studied in this paper is the turbulent boundary layer (TBL).

2.3. TBL excitation

Many authors have developed analytical formulations of the spatial correlation function of TBL excitations from experimental results [7,8]. The model of a correlation function used in this paper was introduced by Corcos:

$$C(x-x',y-y';\omega)=\mathrm{e}^{-\delta_x|x-x'|}\cos(\gamma_x(x-x'))\,\mathrm{e}^{-\delta_y|y-y'|} \tag{18}$$

In this model, x-axis is the direction of the flow. The parameters of the model are derived from measurements and are expressed as follows:

$$\begin{cases}\gamma_{x,y}=\omega/U_c\\ \delta_{x,y}=a_{x,y}\gamma_x+b_{x,y}/\delta\end{cases} \tag{19}$$

U_c is the convection velocity and δ the thickness of the TBL (see Fig. 1). $a_{x,y}$ and $b_{x,y}$ are empirical coefficients. The expression in the wavenumber–frequency domain obtained for TBL excitation is analytically formulated as follows:

$$C(k_x,k_y;\omega)=\frac{\delta_x\delta_y}{\pi^2(\delta_x^2+(\gamma_x-k_x)^2)(\delta_y^2-k_y^2)} \tag{20}$$

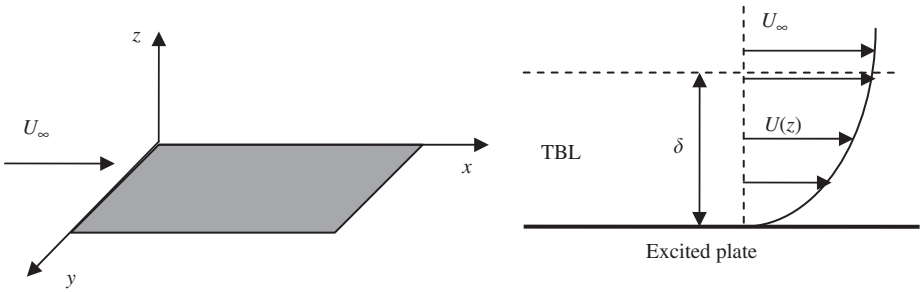

Fig. 1. Turbulent boundary layer excitation.

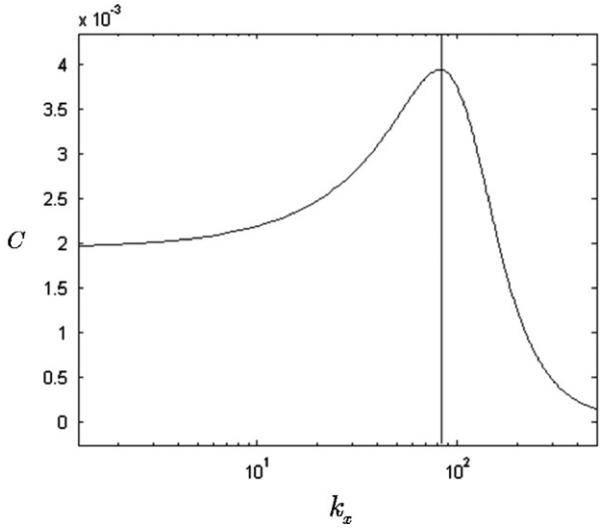

Fig. 2. Spatial correlation C in the direction of the flow for TBL vs wavenumber k_x.

TBL excitation is characterized by an acoustic coincidence effect considering wavenumbers in the direction of the flow. The representation of the spatial correlation function in the wavenumber space highlights the coincidence effect when equality occurs between the structural wavenumber and the acoustical wavenumber (Fig. 2). The coincidence effect in the flow direction corresponds to the maximum and is obtained in the case of $k_x = \gamma_x$.

3. Equivalent ROF excitation

In order to use simplified modal summation expressions, an equivalent spatially de-correlated excitation is introduced here. ROF excitations can be described from general closed formulations of spatially de-correlated functions. For the present applications, the correlation functions are defined in order to use modal basis normalization property:

$$\int_A \Phi_r(x,y)\Phi_s(x,y)\,\mathrm{d}x\,\mathrm{d}y = \delta_{rs} \tag{21}$$

The spatial correlation function is then mass proportional and can be written as

$$C(x-x',y-y';\omega) = C^{\mathrm{eq}}(\omega)\delta(x-x')\delta(y-y') \tag{22}$$

The present approach consists in finding the frequency function $C^{\mathrm{eq}}(\omega)$ that induces the same amount of vibration levels on the structure as a spatially correlated excitation. The function C^{eq} is only dependent on frequency, which implies that the power spectral density obtained for any excitation type is as follows:

$$S_{vv}(x,y;\omega) = \omega^2 \sum_r |\alpha_r(\omega)|^2 \Phi_r^2(x,y) C^{\mathrm{eq}}(\omega) S_{pp}(\omega) \tag{23}$$

From Eq. (13), any spatially correlated excitations can be characterized considering the equivalent point power spectral density:

$$S_{pp}^{\mathrm{eq}}(\omega) = C^{\mathrm{eq}}(\omega) S_{pp}^{\mathrm{rain}}(\omega) \tag{24}$$

Thanks to the previous equation, the vibroacoustic analysis of any structure subjected to acoustic or aerodynamic loads can be performed by exciting the structure with an equivalent ROF load. The developed equivalent model needs to be suited principally in the mid and high frequency ranges. Two approaches are investigated in this paper by expressing the equivalence over the extended physical domain and by expressing the equivalence in the wavenumber space.

3.1. Spatial extent equivalence

The spatial extent equivalence is based on previously published work on estimating vibrations induced by turbulent fluctuations of wall pressure. This work has been presented in [10,11]. The equivalence is made from spatial extent integration of the spatial correlation functions for two different excitations named exc1 and exc2, respectively:

$$\int_\infty \int_\infty \int_\infty C_{\mathrm{exc1}}(\zeta,\chi;\omega)\,\mathrm{d}\zeta\,\mathrm{d}\chi\,\mathrm{d}\omega = \int_\infty \int_\infty \int_\infty C_{\mathrm{exc2}}(\zeta,\chi;\omega)\,\mathrm{d}\zeta\,\mathrm{d}\chi\,\mathrm{d}\omega \tag{25}$$

This relation enables the explicit expression of the equivalent correlation function of the frequency in the form of

$$\int_\infty \int_\infty \int_\infty C^{\mathrm{eq}}(\omega)\delta(\zeta)\delta(\chi)\,\mathrm{d}\zeta\,\mathrm{d}\chi\,\mathrm{d}\omega = \int_\infty \int_\infty \int_\infty C_{\mathrm{exc2}}(\zeta,\chi;\omega)\,\mathrm{d}\zeta\,\mathrm{d}\chi\,\mathrm{d}\omega \tag{26}$$

$$C^{\mathrm{eq}}(\omega) = \int_\infty \int_\infty C_{\mathrm{exc1}}(\zeta,\chi;\omega)\,\mathrm{d}\zeta\,\mathrm{d}\chi \tag{27}$$

As a first analysis of the previous relation, the method will produce relatively low errors for short correlation lengths corresponding to acoustically fast modes. Indeed, space integration being extended to infinity, implicitly implies that the correlation lengths are much smaller than the length of the excited structure.

In Refs. [10,11], the authors justify this approximation when the decay rates of the correlation function are sufficiently high. In other words, results will be accurate in the high frequency limit, as the correlation length decreases with frequency.

3.1.1. Application to an incident reverberant pressure field

For an incident diffuse wall pressure, the spatial extent equivalence leads to the following function:

$$C^{\mathrm{eq}}(\omega) = \int_{\infty}\int_{\infty} \frac{\sin(k_0\zeta)}{k_0\zeta}\frac{\sin(k_0\chi)}{k_0\chi}\,\mathrm{d}\zeta\,\mathrm{d}\chi \tag{28}$$

According to the result

$$\int_0^{\infty} \frac{\sin(t)}{t}\,\mathrm{d}t = \frac{\pi}{2} \tag{29}$$

The equivalent excitation function C^{eq} is expressed by

$$C^{\mathrm{eq}}(\omega) = \frac{\pi^2}{k_0^2} \tag{30}$$

The equivalent ROF excitation to a diffuse incident field involves a simple equivalent function. The previous formulation is applied here to a simply supported aluminum plate excited by an incident diffuse field. The length and width of the plate are $l_x = 2\,\mathrm{m}$ and $l_y = 1.5\,\mathrm{m}$, respectively, and $1.5\times10^{-2}\,\mathrm{m}$ thickness. Validation is made here in terms of the mean joint acceptance functions over resonant modes. The boundary conditions of the simply supported plate lead to analytical formulation of the mode shapes and the joint acceptance functions are

$$j_{mn,rs}(\omega) = \int_A\int_A \sin\left(\frac{m\pi z}{l_x}\right)\sin\left(\frac{r\pi z'}{l_x}\right)\sin\left(\frac{n\pi y}{l_y}\right)\sin\left(\frac{s\pi y'}{l_y}\right)\frac{\sin(k_0(z-z'))}{k_0(z-z')}\frac{\sin(k_0(y-y'))}{k_0(y-y')}\,\mathrm{d}y\,\mathrm{d}y'\,\mathrm{d}z\,\mathrm{d}z' \tag{31}$$

Considering the equivalent ROF excitation, joint acceptance functions are expressed as follows:

$$j_{mn,rs}(\omega) = \frac{\pi^2}{k_0^2}\int_A\int_A \sin\left(\frac{m\pi z}{l_x}\right)\sin\left(\frac{r\pi z'}{l_x}\right)\sin\left(\frac{n\pi y}{l_y}\right)\sin\left(\frac{s\pi y'}{l_y}\right)\delta(z-z')\delta(y-y')\,\mathrm{d}y\,\mathrm{d}y'\,\mathrm{d}z\,\mathrm{d}z' \tag{32}$$

$$j_{mn,rs}(\omega) = \frac{\pi^2}{k_0^2}\frac{A}{4}\delta_{mr}\delta_{ns} \tag{33}$$

Results are plotted from the third octave frequency band 200–2500 Hz (Fig. 3). It can be noticed that the acoustic coincidence frequency, defined as follows, is $f_c = 830\,\mathrm{Hz}$

$$f_c = \frac{c_0^2}{2\pi}\sqrt{\frac{\rho_S}{D}} \tag{34}$$

The mean joint acceptance functions over resonant modes is then well-described based on the ROF excitation equivalent to the incident diffuse field for frequencies higher than the acoustic coincidence frequency. Fig. 3 shows a relatively large error factor below the acoustic coincidence (up to 8 dB for the first frequency band).

The obtained results imply that only acoustically fast modes are well-described using the equivalent ROF excitation obtained from the spatial extent equivalence idea. According to the wavenumber description of an incident diffuse field (17), previous results show that acoustically slow modes have to be taken into account in the entire response of the structure. These considerations are used by Maidanik [6] to developed analytical formulations of radiation efficiency.

3.1.2. Application to TBL excitation

The spatial extent equivalence is here applied to a TBL excitation. TBL excitation is an important source of vibration and noise in the space and aeronautical industry. Most research concerns the definition of the spatial correlation function. The present approach can be applied to any analytical definition of the correlation

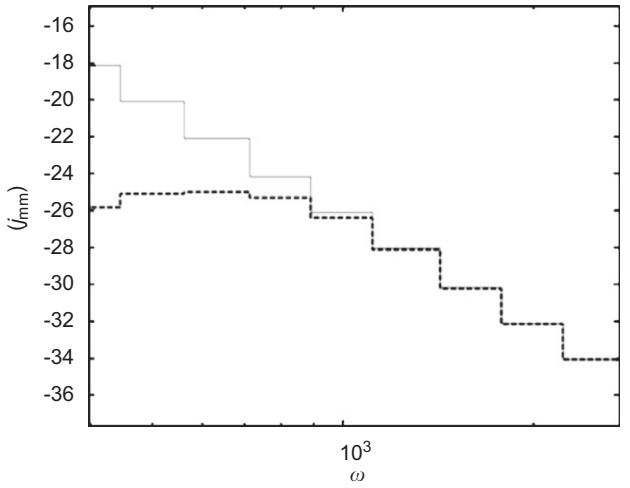

Fig. 3. Mean 'joint acceptance' function over resonant modes $\langle j_{mm} \rangle$ versus frequency: - - analytical, — spatial extent equivalence.

function. The Corcos analytical model is used here. The spatial extent equivalent ROF excitation can then be expressed by

$$C^{\mathrm{eq}}(\omega) = \int_{\infty} \int_{\infty} \mathrm{e}^{-\delta_x|\zeta|} \cos(\gamma_x \zeta)\, \mathrm{e}^{-\delta_y|\chi|}\, \mathrm{d}\zeta\, \mathrm{d}\chi \tag{35}$$

$$C^{\mathrm{eq}}(\omega) = \frac{4\delta_x}{\delta_y(\delta_x^2 + \gamma_x^2)} \tag{36}$$

The numerical application consists of an aluminum plate of 2.8 m length and 1.9 m width, and 5×10^{-3} m thickness. The acoustical coincidence effect is related to the convection speed and to the structural properties. Regarding the response of the structure to a TBL excitation, and considering out-of-plane motion, this coincidence occurs at the critical frequency

$$f_c = \frac{U_c^2}{2\pi} \sqrt{\frac{\rho_s}{D}} \tag{37}$$

where U_c is the convection speed, ρ_s the plate density and D the plate bending stiffness. The present analysis is performed for frequency ranges over the coincidence effect. The convection speed is 75 m/s, and the corresponding coincidence frequency is $f_c = 120$ Hz. Levels are observed in terms of mean square velocity (6) and are averaged over third octave bands in the frequency range 200–5000 Hz.

Fig. 4 shows good agreement between the equivalent ROF mean square velocity levels and the "exact" solution. It can be observed that the discrepancy between the spatial extent equivalence results and the "exact" solution are less than 2 dB for all third octave frequency bands. TBL excitations encountered in the aerospace industry can present convection speeds up to 650 m/s. For such high convection speed, structures are studied either near or far the coincidence effect. The equivalent excitation needs to accurately describe these frequency bands to meet industrial requirements. For the following computation, a convection speed of 270 m/s has been chosen and corresponds to real aerodynamic loading measurements concerning ARIANE 5 wind tunnel testing (Mach 1.2). The coincidence effect occurs at a frequency $f_c = 1540$ Hz. The frequency bands being studied can then correspond to a wide frequency range. Vibration levels observed for third octave frequency bands over the coincidence effect are in agreement with the "exact" solution (Fig. 5). From a physical point of view, the results obtained from this model were foreseeable, since the correlation lengths decrease when the frequency increases. The correlated excitation tends to become spatially delta-correlated in the high frequency limit. This is especially true for the TBL as the correlation lengths have exponential terms, which depend on

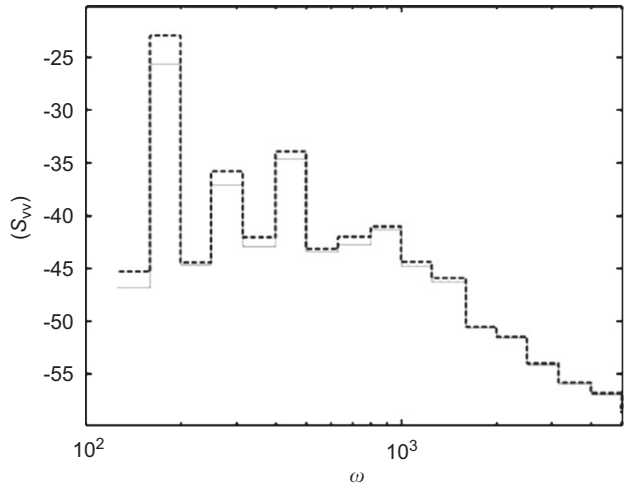

Fig. 4. Mean square velocity in third octave band $\langle S_{vv} \rangle$ versus frequency for $U_c = 75\,\mathrm{m/s}$. — analytical, - - spatial extent equivalence.

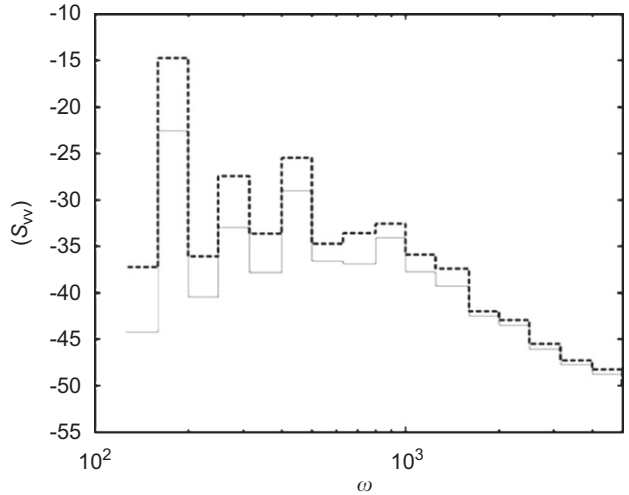

Fig. 5. Mean square velocity $\langle S_{vv} \rangle$ in third octave band versus frequency for $U_c = 270\,\mathrm{m/s}$. — analytical, - - spatial extent equivalence.

the distance between the application points and the frequency. Previous comments concerning the validity of such approach are then verified in this application.

Large errors can be observed for third octave frequency bands below the coincidence effect. Correlation lengths are large here, and the spatial extent equivalence does not represent the real excitation around or below the coincidence effect. Induced discrepancies are over 5 dB around the acoustical coincidence frequency.

The coincidence and high wavenumber regions must then be accurately described from the equivalent spatially de-correlated approach. The interaction between the pressure field and the mode shapes can be observed in the physical domain or in the wavenumber space. The second case gives a convenient representation of the coupling between the modes and the acoustic environment, and leads to relatively simple expressions for correlation functions. In order to highlight the coincidence effect, the equivalent excitations are described hereafter in the wavenumber space.

3.2. Wavenumber space equivalence

The approach proposes an equivalent ROF excitation from a wavenumber-frequency spectrum equivalence. The equivalence can be written in the wavenumber space considering a given wavenumber band. Each wavenumber band can be connected to a given frequency band. The equivalent correlation function can be expressed in the wavenumber space as

$$C^{\mathrm{eq}}(k_x, k_y; \omega) = \frac{C^{\mathrm{eq}}(\omega)}{4\pi^2} \tag{38}$$

Using the wavenumber-frequency spectrum of the excitation under study, and the one of the equivalent ROF excitation, the frequency function C^{eq} can be explicitly as

$$\int_{k=k_1}^{k_2}\int_{\theta=0}^{2\pi} C^{\mathrm{eq}}(k\,\cos(\theta), k\sin(\theta), \omega)k\,\mathrm{d}k\,\mathrm{d}\theta = \int_{k=k_1}^{k_2}\int_{\theta=0}^{2\pi} C(k\,\cos(\theta), k\,\sin(\theta), \omega)k\,\mathrm{d}k\,\mathrm{d}\theta \tag{39}$$

Injecting expression (38) in Eq. (39) leads to

$$C^{\mathrm{eq}}(\omega) = \frac{4\pi}{(k_2^2 - k_1^2)}\int_{k=k_1}^{k_2}\int_{\theta=0}^{2\pi} C(k\,\cos(\theta), k\,\sin(\theta), \omega)k\,\mathrm{d}k\,\mathrm{d}\theta \tag{40}$$

k is the structural wavenumber for the out-of-plane motion, k_1 and k_2 the limit of the given wavenumber band. The equivalent model can be applied to any analytical correlation function in the same way.

3.2.1. Application to an incident reverberant pressure field

According to the expression of the correlation function of an incident diffuse field (17) in the wavenumber space, the equivalence in the wavenumber space can be written as follows:

$$C^{\mathrm{eq}}(\omega) = \frac{\pi^2}{k_0^2} \quad \text{if resonant modes are acoustically fast} \tag{41}$$

$$\text{otherwise} \quad C^{\mathrm{eq}}(\omega) = 0$$

The previous relation and comments in Section 3.1.1 imply that the response of the structure excited by a reverberant diffuse field is well described only for frequency bands over the acoustic coincidence. For frequency bands below the acoustic coincidence, both approaches, spatial extent equivalence and wavenumber equivalence, need to include considerations of the reciprocity between the power radiated in a reverberant field and power injected into a structure from an incident diffuse field.

3.2.2. Application to TBL excitation

It has been shown that the space equivalence approach allows an estimation of the vibration levels of the structure excited by a TBL for a relatively low convection speed. The present equivalence must be able to predict vibration levels above or around the acoustic coincidence effect.

The application of the wavenumber space equivalence for the TBL source gives the equivalent excitation profile:

$$C^{\mathrm{eq}}(\omega) = \frac{4\pi}{(k_2^2 - k_1^2)}\int_{k=k_1}^{k_2}\int_{\theta=0}^{2\pi} \frac{\delta_x\delta_y}{\pi^2(\delta_x^2 + (\gamma_x - k\,\cos(\theta))^2)(\delta_y^2 - k^2\,\sin(\theta)^2)}k\,\mathrm{d}k\,\mathrm{d}\theta \tag{42}$$

Analytical expression of the equivalent function is not of practical interest here and a numerical integration can be performed. A convective speed of 270 m/s, representative of a convective speed appearing at Mach 1.2 in an ARIANE 5 flight was investigated. The numerical application consists of an aluminum plate of 2.8 m length and 1.9 m width, and 5×10^{-3} m thickness. The coincidence frequency is then $f_c = 1540$ Hz, and the frequency range of interest allows us to describe three interesting wavenumber regions (i.e. the low, mid and high wavenumber bands).

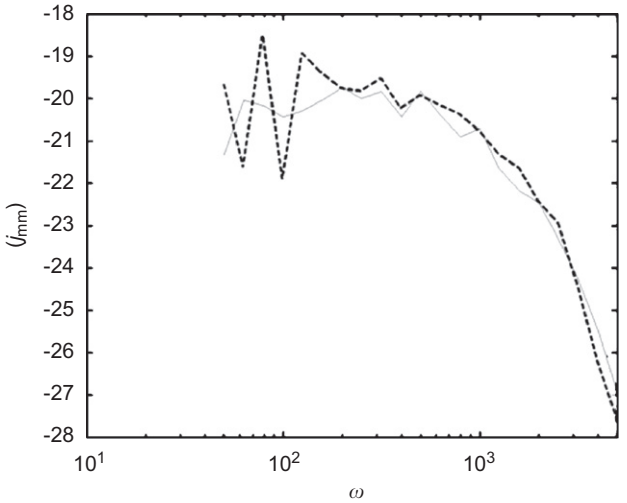

Fig. 6. Mean joint acceptance $\langle j_{mm} \rangle$ in third octave band versus frequency for $U_c = 270$ m/s, - - - - SEALASCAR, -- wavenumber space equivalence.

A first validation was carried out through the comparison of the mean joint acceptance functions of the resonant modes for each third octave frequency band (Fig. 6). The reference value is obtained using an SEA software.[1]

Results show that the equivalent model gives satisfactory results for the joint acceptance averaged over third octave bands in the frequency range 40 Hz to 10 kHz. Errors are lower than 2 dB over the entire frequency range of concern and a good estimate is achieved before and after the coincidence frequency of 1540 Hz. In the first frequency bands, below 200 Hz, the number of modes per third octave band is lower than 10, and the modal overlap is sufficiently low to consider that these frequency bands are the first mid frequency ones.

The equivalent model obtained in the wavenumber space is accurate for mid and high frequency ranges. Vibration levels are estimated here without computing the joint acceptance functions, which can lead to a high cost of CPU time for the mid frequency range.

The comparison of averaged joint acceptances might not be sufficient to prove the validity of the methodology in the mid frequency regime. In order to be more general, the equivalent ROF excitation is validated in terms of power spectral density of velocity (6) without averaging the joint acceptance functions over the resonant modes of the structure (see Fig. 6). Mean square velocity predictions using the wavenumber equivalence seems better than those obtained using the spatial extent ROF equivalent model (see Fig. 7), without any consideration of the acoustic coincidence effect. The deviations observed on averaged values per third octave bands are lower than 2 dB over the entire frequency range studied when the wavenumber equivalence is employed.

This equivalent TBL (ETBL) can then be used over all frequency bands regardless of the acoustic coincidence effect. Fig. 7 shows also that errors in the vibration prediction increase as the frequency decreases. Fig. 8 provides narrow bands mean velocity comparisons.

The previous figure shows that the vibration level is well described in narrow bands as well. Errors on the modal peaks are lower than 2 dB over the entire given frequency range.

As mentioned before, convection speed can reach 650 m/s for aerospace applications, appearing at Mach 3 in an ARIANE 5 flight. For the present structure and frequency range, this convection speed means that all third octave frequency bands are far above the acoustic coincidence effect. Indeed a convection speed of $U_c = 650$ m/s corresponds, for the given structure, to a coincidence frequency $f_c = 9000$ Hz. The previous results in the wavenumber equivalent model showed that the errors introduced in the vibration level

[1]SEALASCAR is an SEA-based code developed and employed by EADS Space Transportation [13,17] for ARIANE vibroacoustic design.

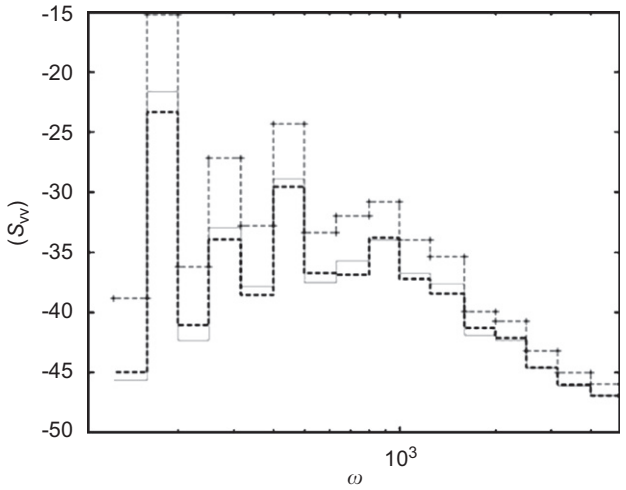

Fig. 7. Mean velocity $\langle S_{vv} \rangle$ in third octave band versus frequency for $U_c = 270$ m/s, - - analytical, — wavenumber equivalence, - + - spatial extent equivalence.

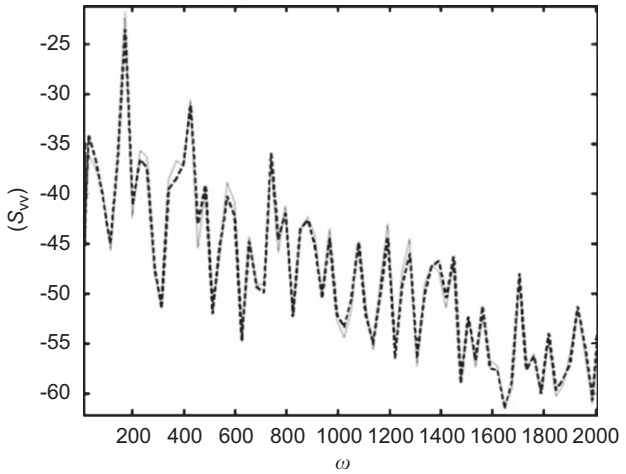

Fig. 8. Mean velocity $\langle S_{vv} \rangle$ in narrow band for $U_c = 270$ m/s, - - - analytical, _ _ _ wavenumber space equivalence.

estimate become larger as the given frequency decreases or, in other words, as the frequency range moves far from the acoustic coincidence effect. This approach is applied to the Mach 3 TBL loading case (see Fig. 9).

Even though the given frequency bands are far below the coincidence effect, results from the ETBL are still relevant. Indeed, the deviation observed is lower than 3 dB for the first and third octave frequency bands and convergence to the exact value occurs in the mid frequency range.

This method is promising because it enables the use of FEM approaches for any correlated excitation case in the mid and high frequency ranges with a relatively low calculation cost. Once the equivalent model is found, the induced vibration levels can be computed without estimating the joint acceptance functions. It can be observed from the previous model that the ROF equivalent excitation does not take into account the structure boundary conditions. Indeed, these boundary conditions are expressed in the integration of the mode shapes over the surfaces of the subsystems. The effect of general boundary conditions is investigated in the following subsection.

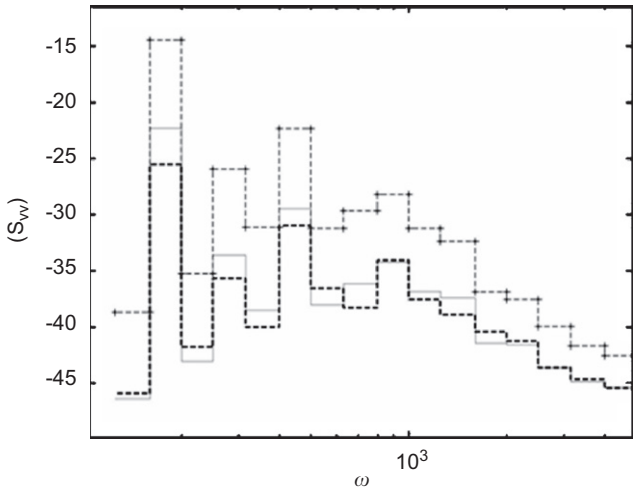

Fig. 9. Mean velocity $\langle S_{vv}\rangle$ in third octave band versus frequency for $U_c = 650$ m/s, - - analytical, — wavenumber equivalence, - + - spatial extent equivalence.

3.3. Influence of boundary conditions

According to what was previously established, equivalent ROF models do not depend on the structural boundary conditions. Indeed, the equivalent correlation function leads to the frequency dependent function removal (from the spatial integrals). In order to validate the generality of these results, the method is applied in what follows to arbitrary boundary conditions, and arbitrary mode shapes functions. In this section, a generic analytical form of modal shapes obtained from an orthogonal basis is first validated. Then, a numerical simulation corresponding to a clamped plate excited by a TBL is considered. This application is investigated through complete FEM of the problem.

A general overview of the influence of the boundary conditions can be obtained using general analytical formulations of the mode shapes of the structure. The present study is carried out on a trigonometric basis and polynomials basis. Combinations of trigonometric functions lead to an orthogonal basis of the mode shapes. The mode shapes of the structure can then be expressed by

$$\phi_{rs}(x,y) = \alpha(\sin(k_r x) + \cos(k_r x)) + \beta(\sin(k_s y) + \cos(k_s y)) \tag{43}$$

α, β are random parameters, r and s the mode's indices in the x and y direction. The "exact" value of the power spectral density of velocity of the structure is then computed using analytical mode shapes to estimate the joint acceptance functions.

The second general analytical expression of the mode shapes refers to a polynomial basis. Two types of orthogonal polynomial basis are employed here. The first is a Legendre polynomial basis. The analytical functions of this family of basis can be expressed as

$$L_1(x) = 1$$

$$L_2(x) = x$$

$$L_{n+1}(x) = \frac{2n+1}{n+1} x L_n(x) - \frac{n}{n+1} L_{n-1}(x), \quad n \geqslant 3 \tag{44}$$

The second general class refers to the Chebichev polynomial basis. This basis is also orthogonal and can be used to represent the modal basis of the structure. The polynomials are then defined by

$$T_1(x) = 1$$

$$T_2(x) = x$$

$$T_{n+1}(x) = 2xT_n(x) - T_{n-1}(x), \quad n \geqslant 3 \tag{45}$$

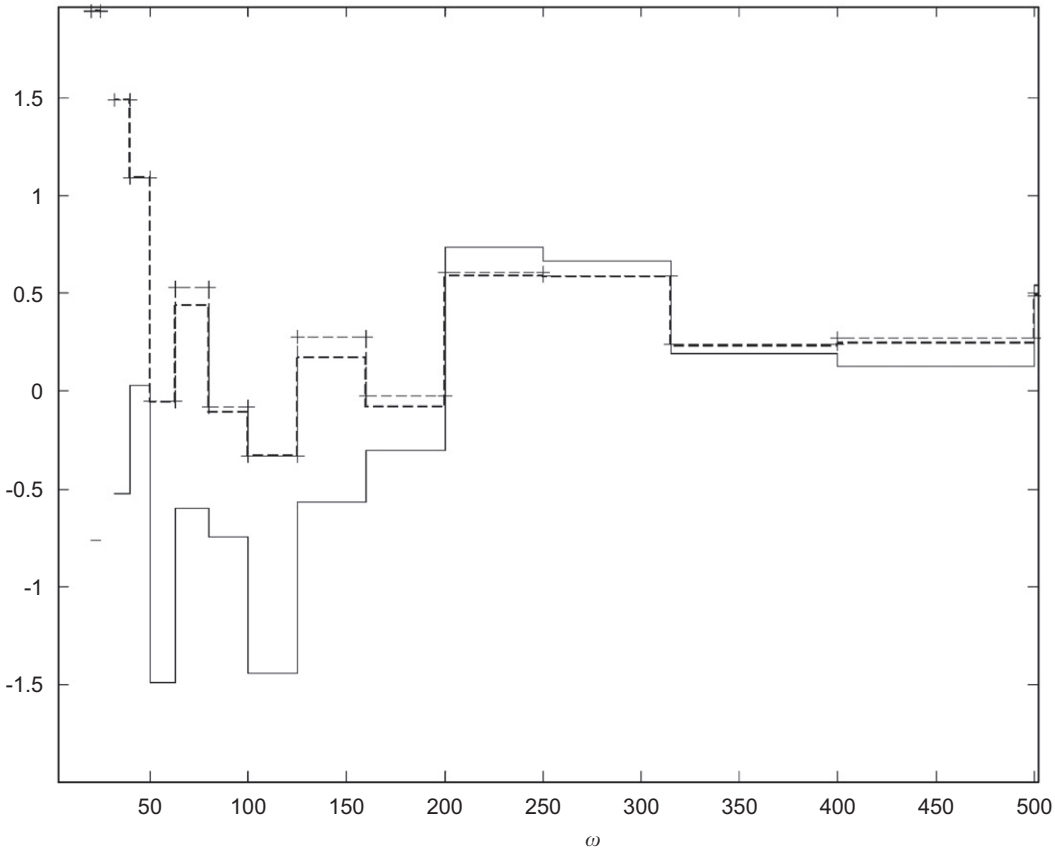

Fig. 10. Error (dB) versus frequency, $U_c = 75\,\mathrm{m/s}$. — Trigonometric basis, -- Legendre polynomial basis, -+- Chebichev polynomial basis.

These two types of polynomial orthogonal basis have been used to validate the equivalent ROF excitation. Results from a random trigonometric basis have been analyzed as well. The structure is the same as in previous sections and is excited with a TBL excitation with a convective speed $U_c = 75\,\mathrm{m/s}$. Results have been compared in terms of difference in dB between "exact" power spectral density of velocity and the one obtained using an equivalent ROF (see Fig. 10).

Fig. 10 shows that the use of the equivalent model leads to errors of the same order in the prediction of the power spectral density of velocity for different boundary conditions. Some discrepancies between the three types of analytical mode shapes can be observed for the first modes of the structure, i.e. in the low frequency band. However, good agreements can be observed in mid and high frequency ranges.

4. Conclusion

An ROF excitation equivalent to acoustic and aerodynamic excitations has been developed and validated in this paper. This approach allows the description of a broadband random spatially correlated excitation from a de-correlated pressure field.

Two methods have been presented here. The first, considers the equivalence over the extended physical domain. It does not meet industrial needs, as it allows equivalent ROF excitation only for frequencies over the acoustic coincidence effect.

A second method has been proposed and validated. It is based on the equivalence definition in the wavenumber space. Validation of the approach has been carried out for different acoustic and aerodynamic excitations, and for different structural boundary conditions. This approach gives acceptable results for a wide

frequency range specifically for turbulent boundary layer excitations. The deviations observed between the equivalent ROF approach and the standard modal analysis using the joint acceptance functions are convenient (for a large scale of convective speed in the case of TBL). In addition, narrow bands results predicting the power spectral density of velocity are very promising. The equivalent ROF excitation has been validated for TBL excitation based on the Corcos model but the present approach can be applied to any analytical correlation function and work on this subject will be pursued. Full scale validation (for a simplified ARIANE 5 vehicle) of what was offered in this paper was already achieved and confirmed the main finding.

References

[1] R.H. Lyon, R. Dejong, *Theory and Application of Statistical Energy Analysis*, second ed., Butterworth-Heinemann, Newton, MA, 1995.
[2] R.S. Langley, P.G. Bremner, A hybrid method for the vibration analysis of complex structural-acoustic systems, *Journal of the Acoustical Society of America* 105 (1999) 1657–1671.
[3] B. Mace, Statistical energy analysis: coupling loss factors, indirect coupling and system modes, *Journal of Sound and Vibration* 279 (1–2) (2005) 141–170.
[4] C.R. Fredö, Statistical Energy Analysis and the Individual Case, PhD Thesis, Chalmers University of Technology, 1995.
[5] B. Hiverniau, Transmissions Solidiennes: Méthodologie de Prévision Vibroacoustique Moyennes et Hautes Fréquences Sous Excitations Aéroacoustiques (Structural Vibration Transmission: Mid-high Frequency Approaches under Aerodynamic Excitations), PhD Thesis, Ecole Centrale de Lyon, 2007.
[6] G. Maidanik, Response of ribbed panels to reverberant acoustic fields, *Journal of the Acoustical Society of America* 34 (6) (1962).
[7] G.M. Corcos, Resolution of pressure in turbulence, *Journal of the Acoustical Society of America* 35 (2) (1963).
[8] D.M. Chase, Modelling the wavevector–frequency spectrum of turbulent boundary layer wall-pressure, *Journal of Sound and Vibration* 70 (1980) 29–67.
[9] S. Finnveden, F. Birgersson, U. Ross, T. Kremer, A model of wall pressure correlation for prediction of turbulence-induced vibration, *Journal of Fluids and Structures* 20 (2005) 1127–1143.
[10] G. Maidanik, Use of delta function for the correlations of pressure fields, *Journal of the Acoustical Society of America* 33 (11) (1961) 1598–1606.
[11] J. Park, T. Siegmund, L. Mongeau, Analysis of the flow-induced vibrations of viscoelastically supported rectangular plates, *Journal of Sound and Vibration* 261 (2003) 225–245.
[12] S.J. Elliot, P. Gardonio, C. Maury, A feasibility study for the laboratory simulation of turbulent boundary layer pressure fields, *Seventh AIAA/CEAS Aeronautics Conference*, 28–30 May 2001, Maastricht, Netherlands.
[13] Troclet, B., *Manuel théorique LASCAR*, EADS Launch Vehicles, 1987.
[14] C. Maury, P. Gardonio, S.J. Elliot, A wavenumber approach to modeling the response of a randomly excited panel. Part I: general theory, *Journal of Sound and Vibration* 252 (1) (2002) 83–113.
[15] F. Birgersson, S. Finnveden, A spectral element for modeling of plate vibration. Part 2: turbulence excitation, *Journal of Sound and Vibration* 287 (2005) 315–328.
[16] S.A. Hambric, Y.F. Hwang, W.K. Bonness, Vibrations of plates with clamped and free edges excited by low-speed turbulent boundary layer, *Journal of Fluids and Structures* 19 (2004) 93–110.
[17] S. De Rosa, F. Franco, Exact and numerical responses of a plate under a turbulent boundary layer excitation, *Journal of Fluids and Structures* 24 (2008) 212–230.
[18] B. Troclet, M. Depuydt, P. Gonzalez. Experimental analysis of the aerodynamic noise on the Ariane 5 Launch Vehicle Upper Part, *Ariane 5 Structures et Technologies*, Cépaduès-Editions, 1993, pp. 515–526.